Hydrogen Bonding and Reactivity Behavior of Guanosine-5′ -Diphosphate from DFT and Molecular Docking Approach

Manoj Kumar Chaudhary[1]*, Bhupendra Maharjan[1], Gulab Singh Verma[2], Rajesh Kumar Shukla[2]

[1]*Department of Physics, Tribhuvan University, Amrit Campus, Institute of Science and Technology, Kathmandu 44600, Nepal*
[2]*Department of Physics, University of Lucknow, Lucknow-226007, India*

Research Article

ISSN: 3059-9504 (online)

Article History

Received: November 28, 2024
Revised: December 15, 2024
Accepted: December 17, 2024
Published: December 28, 2024

Keywords

Guanosine-5′ -Diphosphate (GDP), MEP, DFT, Molecular Docking, Global Reactivity Descriptor

***Corresponding author**
Email: *manoj.chaudhary@ac.tu.edu.np*
Orcid: 0000-0002-49351827 (M.K. Chaudhary)
Phone: + 977-9841436728

ABSTRACT

Minimum energy structure of Guanosine-5′-Diphosphate (GDP) has been obtained from DFT-B3LYP/6-311++G(d,p) level of theory. The intermolecular hydrogen bonding possibility of GDP has been predicted from optimized parameters, MEP surface analysis and molecular docking approach. The hyper conjugative interaction energy has been analyzed from NBO approach and the significant interaction energy for stability of the molecule is the delocalization of lone pair electron η (1) C21→ π*(N18–C30) and yields 271.82 kcal/mol energy. For the ligand protein interaction, the protein Cdc42 is predicted for the ligand GDP and the three PDB codes 1ANO, 1A4R and 1DOA has been taken into consideration. The Inhibition constant for 1DOA is least which emphases the most binding energy -7.2 kcal/mol. The MEP surface analysis exhibits the most negative potential across O31 and N20 whereas the positive potential cloud is seen across the hydroxyl groups (O8-H9, O3-H4, O35-H36) and amine groups (N26-H_2, N23-H). These regions have significant roles in hydrogen bonding which is satisfied from the molecular docking approach.

1. INTRODUCTION

Guanosine-5′ -Diphosphate (GDP) is a nucleoside diphosphate which consists of a pyrophosphate group, a pentose sugar ribose and the nucleobase guanine [1]. The chemical formula of GDP is $C_{10}H_{15}N_5O_{11}P_2$. It is prepared from condensation of the hydroxy group at the 5′ position of quanosine with pyrophosphoric acid. GDP is the uncoupling inhibitor as well as Escherichia coli metabolite and mouse metabolite. According to its biological activity it lies in Homo sapiens, Escherichia coli and other organism [2-4]. The anti-bacterial activity of Guvermectin (GV) with Guanosine-5′ -Monophosphate (GMP) was studied from molecular docking, genetic and biochemical approach [5]. Guanosine-5′ -Triphosphate (GTP) exhibit the good binding behavior with the many proteins like: NS3, NS4A and NS5 by analyzing from AutoDockVina [6].

The geometry optimization, binding sites and molecular docking with Cell division control protein 42 homolog (Cdc42) of GDP have not been performed in the literature. In this manuscript we have focused on these properties of GDP from density functional theory (DFT) and molecular docking approach.

2. METHODS AND METHODOLOGY

The geometry optimization has been carried out from quantum chemical calculation by using Gaussian 16 software [7] from DFT approach by using the hybrid functional B3LYP [8-11] with 6-311++G(d,p) basis set [12]. The GausssView 06 [13] software is implemented to visualize the optimized parameter to study the distribution of charge around the molecule from molecular electrostatic potential (MEP) surface and charge on the orbital lob in highest occupied molecular orbital (HOMO) and lowest unoccupied molecular orbital (LUMO). The natural bond orbital (NBO) analysis is studied from NBO 3.1 which is included in Gaussian 16 software [14]. The binding activity of GDP with the protein codes 1ANO, 1A4R and 1DOA have been examined from AutoDock Tools and Discovery Studio Visualizer 4.5 [15, 16].

3. RESULTS AND DISCUSSION

3.1 Geometry Optimization

The compound GDP has been optimized from DFT/B3LYP/6-311++G(d,p) and the 3D least energy structure with atoms labeling of GDP is presented in Fig. 1. The minimum energy was calculated as 1364642.78 kcal/mol. The optimized parameters of GDP such as: bond length and bond angles are depicted in Table 1. The least value of bond length has been obtained across O35-H36, O3-H4, and O8-H9 and their respective values are 0.962, 0.966 and 0.966 Å. This least values of bond length are due to high positive potential analyzed from MEP and these regions have prominent role in hydrogen bonding. Similarly, the longest bond length was found across O5-P6 and its value is 1.647 Å. This is due to intra molecular hydrogen bonding across O2-H11. The least value of angle was obtained across O3-P1-O12 and its value is 99.815° this is also due to interamolecular hydrogen bonding across O2-H11. The highest bond angle is obtained across C21-C22-O31 and its value is 131.379°, this is due to high negative potential across O31 and it takes part in intermolecular hydrogen bonding which is satisfied by molecular docking and MEP surface analysis.

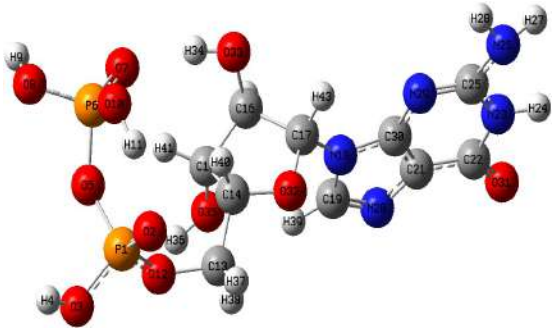

Fig. 1: 3D optimized structure of Guanosine-5′ -Diphosphate with atoms numbering from B3LYP/6-311++G(d,p).

Table 1: Optimized parameters (bond length and bond angle) of Guanosine-5′ -Diphosphate from B3LYP/6-311++G(d,p).

Bond Length	(Å)
R(P1–O2)	1.486
R(P1–O3)	1.590
R(P1–O5)	1.628
R(P1–O12)	1.577
R(O3–H4)	0.966
R(O5–P6)	1.647
R(P6–O7)	1.477
R(P6–O8)	1.595
R(P6–10)	1.578
R(O8–H9)	0.966
R(O10–H11)	0.988
R(O12–C13)	1.467
R(C13–C14)	1.518
R(C13–H37)	1.089
R(C13–H38)	1.087
R(C14–C15)	1.538
R(C14–O32)	1.424
R(C14–H40)	1.099
R(C15–C16)	1.535
R(C15–O35)	1.425
R(C15–H41)	1.090
R(C16–C17)	1.553
R(C16–O33)	1.419
R(C16–H42)	1.093
R(C17–N18)	1.445
R(C17–O32)	1.441
R(C17-H43)	1.090
R(N18–C19)	1.394
R(N18–C30)	1.378
R(C19–N20)	1.304
R(C19–H39)	1.078
R(N20–C21)	1.381
R(C21–C22)	1.437
R(C21–C30)	1.391
R(C22–N23)	1.440
R(C22–O31)	1.215
R(N23–H24)	1.012
R(N23–C25)	1.369
R(C25–N26)	1.377
R(C25–N29)	1.308
R(N26–H27)	1.009
R(N26–H28)	1.010
R(N29–C30)	1.356
R(O33–H34)	0.970
R(O35–H36)	0.962
Bond Angle (°)	
A(O2–P1–O3)	118.465
A(O2–P1–O5)	109.874
A(O2–P1–O12)	117.830
A(O3–P1–O5)	103.112
A(O3–P1–O12)	99.815
A(O5–P1–O12)	106.069
A(P1–O3–H4)	114.487
A(P1–O5–P6)	131.209
A(O5–P6–O7)	111.642
A(O5–P6–O8)	102.479
A(O5–P6–10)	104.429
A(O7–P6–O8)	114.210
A(O7–P6–10)	119.290
A(O8–P6–10)	102.986
A(P6–O8–H9)	112.482
A(P6–10–H11)	114.386
A(P1–O12–C13)	124.021
A(O12–C13–C14)	109.827
A(O12–C13–H37)	109.392
A(O12–C13–H38)	104.751
A(C14–C13–H37)	111.460
A(C14–C13–H38)	111.077
A(37–C13–H38)	110.114
A(C13–C14–C15)	116.134
A(C13–C14–O32)	107.658
A(C13–C14–H40)	109.588
A(C15–C14–O32)	105.214
A(C15–C14–H40)	108.474
A(O32–C14–H40)	109.574
A(C14–C15–C16)	99.942
A(C14–C15–O35)	112.890
A(C14–C15–H41)	112.728
A(C16–C15–O35)	109.057
A(C16–C15–H41)	110.858
A(O35–C15–H41)	110.846
A(C15–C16–C17)	103.642
A(C15–C16–O33)	111.260
A(C15–C16–H42)	111.554
A(C17–C16–O33)	106.217
A(C17–C16–H42)	112.172
A(O33–C16–H42)	111.613
A(C16–C17–N18)	116.410
A(C16–C17–O32)	105.998
A(C16–C17–H43)	108.813
A(N18–C17–O32)	109.563
A(N18–C17–H43)	106.355
A(O32–C17–H43)	109.618
A(C17–N18–C19)	129.319
A(C17–N18–C30)	124.843
A(C19–N18–C30)	105.744
A(N18–C19–N20)	112.965
A(N18–C19–H39)	120.728
A(N20–C19–H39)	126.306
A(C19–N20–C21)	105.007
A(N20–C21–C22)	130.438
A(N20–C21–C30)	110.667
A(C22–C21–C30)	118.892
A(C21–C22–N23)	109.520
A(C21–C22–O31)	131.379
A(N23–C22–O31)	119.100
A(C22–N23–H24)	113.548
A(C22–N23–C25)	126.344
A(H24–N23–C25)	119.984
A(N23–C25–N26)	116.999
A(N23–C25–N29)	123.328
A(N26–C25–N29)	119.629
A(C25–N26–H27)	117.881
A(C25–N26–H28)	113.448
A(H27–N26–H28)	114.438
A(C25–N29–C30)	113.100
A(N18–C30–C21)	105.613
A(N18–C30–N29)	125.575
A(C21–C30–N29)	128.803
A(C14–O32–C17)	109.305
A(C16–O33–H34)	110.931
A(C15–O35–H36)	109.010

3.2 Molecular Electrostatic Potential (MEP) Surface Analysis

The distribution of charge in the molecular system is not uniform and its presence around the compound is visualized in terms of pictorial presentation by using MEP surface analysis. The color codes identify the potential due to charge. The red region for most negative potential, green one for zero potential whereas the blue one for positive potential. The potential increases in terms of color as red > yellow > green > blue. The molecular electrostatic potential due to combined effect of electrons and protons in the molecular system is given by the formula [17, 18].

$$V(r) = \sum_{A} \frac{Z_A}{\left|\overrightarrow{R_A} - \vec{r}\right|} - \int \frac{\rho\left(\overrightarrow{r'}\right)}{\left|\overrightarrow{r'} - \vec{r}\right|}$$

Where $\rho(r')$ stands for negative concentration and Z_A is the positive charge concentration on nucleus A, present at R_A.

The MEP surface of GDP is presented in Fig. 2. The most negative potential in GDP was found across O31 and N20 after that certain negative cloud was seen across O2, O7, O32 and O33. These reasons have prominent participation in hydrogen bonding as well as reactive sites.

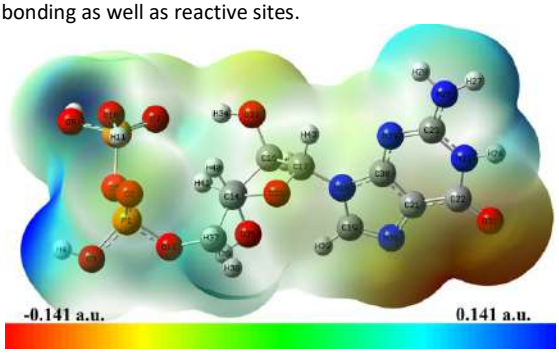

Fig. 2: MEP surface of Guanosine-5′-Diphosphate.

This is verified by molecular docking in section 3.5. Similarly, the positive cloud has been fond across the hydroxyl groups (O8-H9, O3-H4, O35-H36) and amine groups (N26-H_2, N23-H). These functional groups has wide role to take part in chemical reaction as well as in hydrogen bonding. This is also satisfied by molecular docking analysis, explained in molecular docking in section 3.5.

3.3 Natural Bond Orbital (NBO) Analysis

NBO analysis is the significant tool to study the stability of compound in terms of delocalization of charge from donor (i) to acceptor (j) orbitals. The concentration of charge in the donor orbital ED(i)/e is more than the concentration of charge in acceptor orbital ED(j)/e. The electron in the molecular system delocalized from higher concentration to lower concentration and gains the stability. The stability is measured in terms of stabilization energy E(2) and is given by the formula [19,20]

$$E(2) = E(i,j) = -q_i \left[\frac{F_{i,j}^2}{E_i - E_j}\right]$$

Where E_i is the energy of (i) orbital and E_j is the energy of (j) orbital, $F_{i,j}$ is the off-diagonal element of Fock matrix and q_i is the occupancy of NBO.

The stabilization energy E(2) when the electron delocalized from donor (i) to acceptor (j) orbital along with electron density of donor and acceptor orbital for GDP is presented in Table 2. The stability of GDP is due to delocalization of charge from $\sigma \rightarrow \sigma^*$, $\pi \rightarrow \pi^*$ and from LP orbital $\eta \rightarrow \pi^*$ and σ^*.The delocalization of charge from η(1) C21→ π*(N18-C30) and π*(C22-O31) stabilizes the GDP significantly with respective stabilization energy 271.82 and 89.23 kcal/mol. Similarly, the others prominent transitions are π (C25-N29) → π*(N18-C30) and π (N18-C30) → π*(C19-N20) with stabilization energy 32.62 and 23.47 kcal/mol respectively. The remaining transitions are presented in Table 2.

Table 2: Stabilization energy E(2), electron density of donor ED(i)/e and acceptor ED(j)/e orbitals of GDP from B3LYP/6-311++G(d,p) level of theory.

Donor NBO (i)	ED(i)/e	Acceptor NBO (j)	ED(j)/e	E(2) kcal/mol	E(j)-E(i) a.u.	F(i,j) a.u.
σ(N29–C30)	1.97757	σ*(C25–N26)	0.03056	5.41	1.24	0.073
σ(N26–H28)	1.98642	σ*(N23–C25)	0.04918	5.27	1.11	0.069
σ(C25–N29)	1.97916	σ*(N18–C30)	0.04158	5.17	1.32	0.074
σ(C21–C30)	1.97244	σ *(C17–N18)	0.04858	5.39	1.05	0.067
σ(C19–N20)	1.98322	σ *(C21–C22)	0.06324	5.00	1.34	0.074
σ(N18– C19)	1.98426	σ *(N29–C30)	0.01977	5.07	1.29	0.072
σ(C17– H43)	1.97543	σ *(N18–C19)	0.04370	5.69	0.94	0.066
π (C25–N29)	1.83879	π*(N18–C30)	0.71341	32.63	0.29	0.102
π (C19–N20)	1.89207	π*(N18–C30)	0.71341	6.26	0.26	0.043
π (N18–C30)	1.84422	σ*(C17–O32)	0.04765	8.65	0.60	0.066
π (N18–C30)	1.84422	π*(C19–N20)	0.29151	23.47	0.36	0.085
η (3) O 7	1.80654	σ*(O5–P6)	0.20849	25.87	0.46	0.097
η (3) O 7	1.80654	σ(P6–O10)	0.15182	10.67	0.53	0.068
η (3) O 2	1.80720	σ*(P1–O3)	0.15661	20.47	0.51	0.092
η (3) O 2	1.80720	σ*(P1–O12)	0.15707	14.59	0.52	0.079
η (2) O10	1.90864	σ*(P6–O7)	0.09341	10.97	0.71	0.079

η (2) O10	1.90864	σ*(P6–O8)	0.15436	7.12	0.57	0.058
η (2) O 8	1.91490	σ*(O5–P6)	0.20849	12.15	0.53	0.074
η (2) O 7	1.81388	σ*(P6–O8)	0.15436	22.77	0.51	0.097
η (2) O 7	1.81388	σ*(P6–O10)	0.15182	11.17	0.53	0.069
η (2) O 5	1.90273	σ*(P1–O12)	0.15707	8.35	0.61	0.065
η (2) O 5	1.90273	σ*(P6–O7)	0.09341	6.96	0.75	0.064
η (2) O 3	1.91712	σ*(P1–O2)	0.09512	7.41	0.71	0.065
η (2) O 3	1.91712	σ*(P1–O5)	0.20259	10.24	0.55	0.069
η (2) O 2	1.81301	σ*(P1–O5)	0.20259	25.01	0.49	0.099
η (2) O 2	1.81301	σ*(P1–O12)	0.15707	8.80	0.53	0.062
η (2) O 2	1.81301	σ*(O10–H11)	0.03570	11.28	0.70	0.083
η (2) O35	1.95584	σ*(C14–C15)	0.04816	8.37	0.67	0.067
η (2) O33	1.94855	σ*(C16–H42)	0.03294	8.60	0.70	0.069
η (2) O32	1.91580	σ*(C14–H40)	0.03590	8.06	0.69	0.067
η (2) O32	1.91580	σ*(C17–N18)	0.04858	5.64	0.66	0.055
η (2) O32	1.91580	σ*(C17–H43)	0.02719	5.49	0.72	0.057
η (2) O31	1.84655	σ*(C21–C22)	0.06324	16.98	0.74	0.102
η (2) O31	1.84655	σ*(C22–N23)	0.09970	32.16	0.60	0.126
η (2) O12	1.89372	σ*(P1–O5)	0.20259	13.13	0.54	0.077
η (1) O 8	1.96615	σ*(P6–O7)	0.09341	5.23	1.01	0.066
η (1) O 5	1.93975	σ*(P1–O2)	0.09512	5.19	0.92	0.062
η (1) N29	1.89453	σ*(C21–C30)	0.03940	8.54	0.93	0.081
η (1) N29	1.89453	σ*(N23–C25)	0.04918	12.83	0.80	0.092
η (1) N26	1.82065	π*(C25–N29)	0.40604	36.51	0.31	0.101
η (1) N23	1.64915	π*(C22–O31)	0.33643	40.24	0.30	0.099
η (1) N23	1.64915	π*(C25–N29)	0.40604	61.09	0.27	0.116
η (1) C21	1.13946	π*(N18–C30)	0.71341	271.82	0.07	0.128
η (1) C21	1.13946	π*(C19–N20)	0.29151	48.48	0.13	0.084
η (1) C21	1.13946	π*(C22–O31)	0.33643	89.23	0.14	0.115
η (1) N20	1.92308	σ*(N18–C19)	0.04370	8.32	0.77	0.072
η (1) N20	1.92308	σ*(C21–C30)	0.03940	5.61	0.92	0.065
η (1) O12	1.94323	σ*(P1–O2)	0.09512	7.36	0.92	0.074

3.4 Frontier Molecular Orbital (FMO's) and Global Reactivity Descriptor

The FMO's have the prominent role to take part in chemical reaction in the molecular system. The highest occupied molecular orbital (HOMO) has the major role to donate the electrons whereas the lowest unoccupied molecular orbital (LUMO) has significant role to absorb the electrons. The HOMO-LUMO energy (ΔE_{L-H}) determines the stability of the compound. Higher the value of (ΔE_{L-H}) more the stability of the compound and less the value of ΔE_{L-H}.the compound is more reactive. The HOMO-LUMO plot of GDP with TD-B3LYP/6-311++G(d,P) is presented in Fig. 3. In HOMO the concentration of charge is found across amine group $N26H_2$, imidazole as well as benzene rings, but in LUMO this charges is diverges to carbonyl group C22=O31 and to the benzene and imidazole rings. These regions have significant role in hydrogen bonding as well as ligand protein binding interaction which is also justified in section 3.5.

The HOMO energy (E_L), LUMO energy (E_H), the value of ΔE_{L-H}, electronegativity (χ), softness (S), hardness (η), electrofilicity index (ω), value of chemical potential (μ) for GDP is depicted in Table 3. These values is calculated in terms of E_H and E_L and is given by the formulae [17, 21].

$$\chi = -\frac{1}{2}(E_H + E_L)$$

$$\mu = -\chi = \frac{1}{2}(E_H + E_L)$$

$$\eta = \frac{1}{2}(E_L - E_H)$$

$$S = \frac{1}{2\eta}$$

$$\omega = \frac{\mu^2}{2\eta}$$

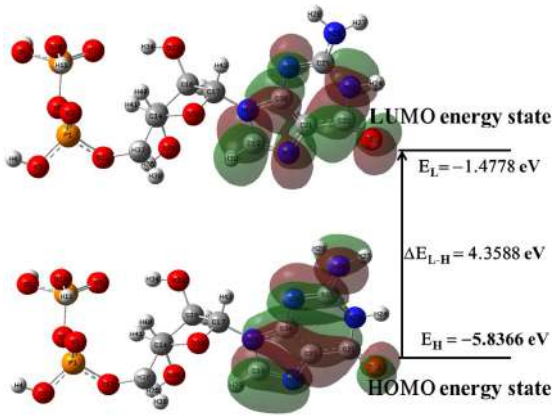

Fig. 3: HOMO -LUMO plot of Guanosine-5′-Diphosphate.

Table 3: Calculated values of E_H, $E_L(\Delta E_{L-H}$, χ, S, η, ω, μ from B3LYP/6-311++G(d,p) of Guanosine-5′-Diphosphate.

E_H (eV)	E_L(eV)	($E_L - E_H$) (eV)	χ(eV)	μ(eV)	η(eV)	S(eV^{-1})	ω(eV)	ΔNmax
-5.8366	-1.4778	4.3588	3.6572	-3.6572	2.1794	0.2294	3.0685	1.6781

3.5 Molecular Docking

Molecular docking is the essential tool to identify the binding of ligand with predicted target protein. The target protein of GDP which is unique ligand of Cell division control protein 42 homolog (Cdc42) is predicted from the Swiss Target Prediction [22]. The three PDB codes 1ANO, 1A4R and 1DOA have been downloaded from the RCSB data bank [23] and proteins have been cleaned by removing the water molecules and docked ligand by using Discovery Studio Visualizer 4.5 [16]. After that the docking has been performed by AutoDock Tools and the docked conformers have been visualized from Discovery Studio Visualizer 4.5. Out of the many docked conformer the only best conformers are presented in Fig. 4 and the 2-D structure of docked conformers is depicted in Fig. 5. The conventional hydrogen bond, inhibition constant, ligand efficiency and the binding atoms of GDP is presented in Table 4. Generally the atoms O2, O3, O5, O7, O33, O35, H4,H11, H24, H28, and H34 binds with residue of protein Cdc42. These atoms are also predicted in geometry optimization and MEP surface analysis in sections 3.1 and 3.2. Out of three PDB codes the 1DOA has highest binding energy -7.2 kcal/mol. The protein Cdc42 shows the good inhibitor for GDP.

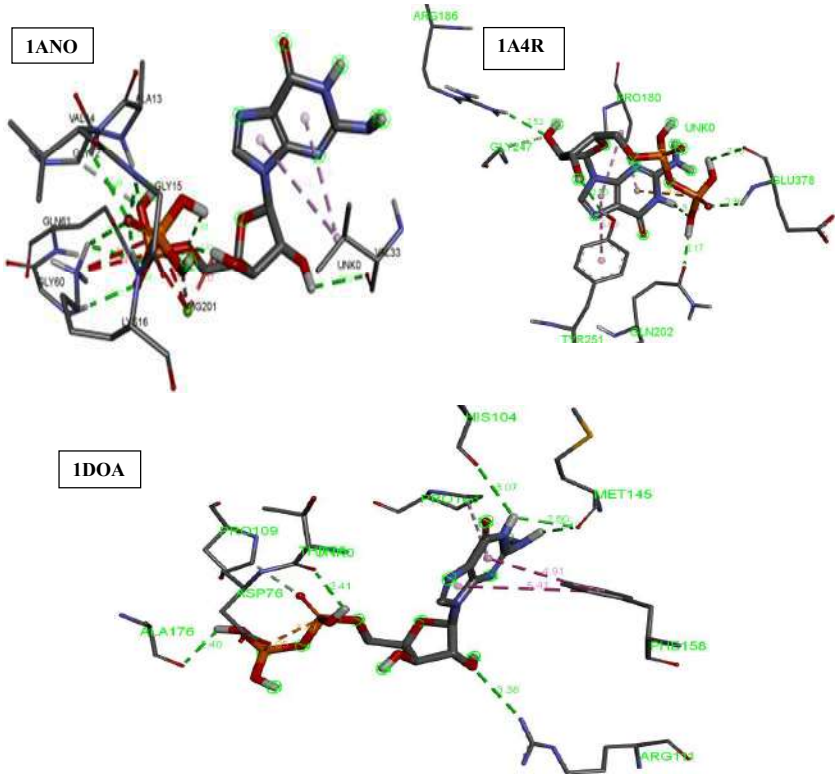

Fig. 4: Residues of amino acids with ligand Guanosine-5′ -Diphosphate.

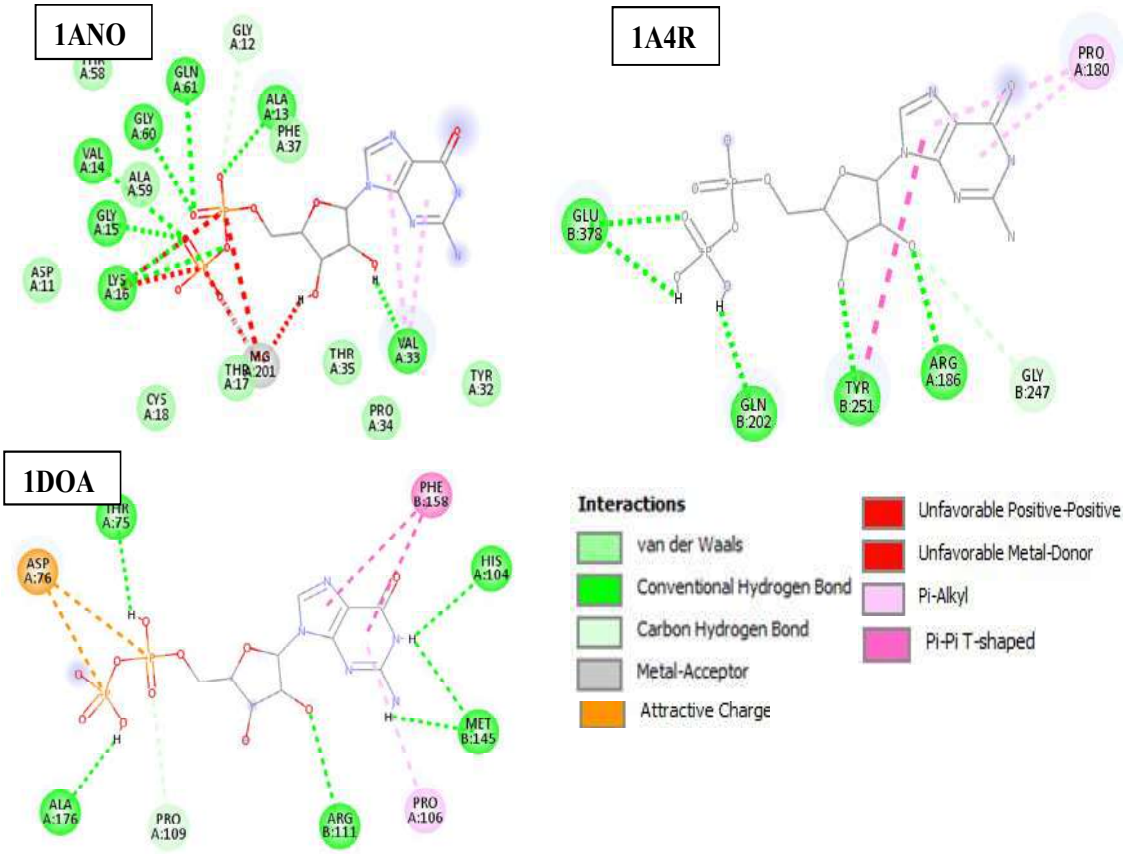

Fig. 5: 2 D structures of docked conformers with ligand Guanosine-5' -Diphosphate.

Table 4. Molecular docking parameters of Guanosine-5' -Diphosphate with protein code 1ANO, 1A4R and 1DOA of Cell division control protein 42 homolog.

Ligand	Protein	PDB code	Bond length (Å)	Binding Atoms	Amino acid	Binding energy (kcal/mol)	Inhibition constant (μM)	Ligand efficiency
GDP	Cdc42	1ANO	2.50	H34	VAL A:33	− 6.6	14.35	−0.24
			2.68	O3	ALA A:13			
			2.68	O2	GLN A:61			
			2.41	O2	GLY A:60			
			2.41	O7	VAL A:14			
			2.15	O7	GLY A:15			
			2.13	O7,O5	LYS A:16			
		1A4R	2.52	O33	ARG A:186	−6.6	14.35	−0.24
			2.50	O35	TIR B:251			
			2.17	H11	GLN B:202			
			2.36	O7	GLU B:378			
			2.76	H9	GLU B:378			
			3.07	H24	HIS A:104			
		1DOA	2.60	H24	MET B:145	−7.2	5.21	−0.26
			2.18	H28	MET B:145			
			3.38	O33	ARG B:111			
			2.41	H4	THR A:75			
			2.40	H11	ALA A:176			

4. CONCLUSIONS

The three dimensional optimized structure of GDP has been obtained from DFT-B3LYP/6-311++G(d,p) and the optimized energy is calculated as 1364642.78 kcal/mol. The least bond length is calculated as 0.962 and 0.966 Å across (O35-H36) and (O3-H4). These moieties will take part in inermolecular hydrogen bonding. The longest bond length is calculated as 1.647 Å across (O5-P6). This is due to intramolecular hydrogen bonding across (O2-H11). MEP analysis conformed that the concentration of negative charge is more across O2, O7, O32 and O33. These moieties have prominent role to take part in hydrogen bonding as well as reactive sites in molecular docking. Moreover, the positive concentration of charge in GDP is most across the hydroxyl groups (O8-H9, O3-H4, O35-H36) and amine groups (N26-H_2, N23-H). These regions have maximum possibility to take part in hydrogen bonding which is justified by molecular docking. The HOO-LUMO energy gap is obtained as 4.3588 eV, chemical potential is obtained as -3.6572 eV. The highest binding energy -7.2 kcal/mol is found across PDB code 1DOA of protein Cdc42. The atoms which bind with residue of amino acid are O2, O3, O5, O7, O33, O35, H4, H11, H24, H28, and H34 which is also justified from geometry optimization and MEP analysis.

AUTHOR CONTRIBUTION

M.K. Chaudhary: Conceptualization of research activity, data analysis and manuscript writing; B. Maharjan: Analysis, and drafting; G. S. Verma: Data calculation R. K. Shukla: supervision and editing.

DECLARATIONS CONFLICT OF INTEREST

The authors declare no competing interests.

REFERENCES

[1] L.E. Bettio, J. Gil-Mohapel, A.L. Rodrigues. “Guanosine and its role in neuropathologies. Purinergic Signal” 2016 Sep;12(3):411-26. Epub 2016 Mar 22. PMID: 27002712; PMCID: PMC5023624. https://doi.org/10.1007/s11302-016-9509-4

[2] National Center for Biotechnology Information. "PubChem Compound Summary for CID 135398619, Guanosine Diphosphate *PubChem*, https://pubchem.ncbi.nlm.nih.gov/compound/Guanosine-Diphosphate. Accessed 1 December, 2024.

[3] M.F., Carlier, Guanosine-5’-triphosphate hydrolysis and tubulin polymerization. *Molecular and cellular biochemistry,* **47** (1982): 97-113. https://doi.org/10.1007/BF00234410

[4] N. Nemoto, S. Baba, G. Kawai, and G.Sampei. Crystal structure of guanosine 5’-monophosphate synthetase from the thermophilic bacterium Thermus thermophilus HB8. *Structural Biology and Crystallization Communications* 80, no. 10 (2024). doi.org/10.1107/S2053230X2400877X

[5] M. Zhang, L. Lei, L. Cheng, M. Aifang, L. Junzhou, Y. Chenyu, C. Xujun. Natural product guvermectin inhibits guanosine 5’-monophosphate synthetase and confers broad-spectrum antibacterial activity. *International Journal of Biological Macromolecules,* **267** (2024): 131510. https://doi.org/10.1016/j.ijbiomac.2024.131510

[6] D. K. Shill, J. Shafina, M. A. Mohammad Mamun, B. L. Hasan, M. Alam, Z. Rahman, and M. Rahman. S-Adenosyl-l-homocysteine exhibits potential antiviral activity against dengue virus serotype-3 (DENV-3) in Bangladesh: a viroinformatics-based approach. *Bioinformatics and Biology Insights,* 17 (2023): 11779322231158249. https://doi.org/10.1177/11779322231158249

[7] M.J. Frisch, G.W. Trucks, H.B. Schlegel, G.E. Scuseria, M.A. Robb, J.R. Cheeseman, G. Scalmani, V. Barone, B. Mennucci, G.A. Petersson, H. Nakatsuji, M. Caricato, X. Li, H.P. Hratchian, A.F. Izmaylov, J. Bloino, G. Zheng, J.L. Sonnenberg, M. Hada, M. Ehara, K. Toyota, R. Fukuda, J. Hasegawa, M. Ishida, T. Nakajima, Y. Honda, O. Kitao, H. Nakai, T. Vreven, J.A. Montgomery, J.E. Peralta, F. Ogliaro, M. Bearpark, J.J. Heyd, E. Brothers, K.N. Kudin, V.N. Staroverov, R. Kobayashi, J. Normand, K. Raghavachari, A. Rendell, J.C. Burant, S.S. Iyengar, J. Tomasi, M. Cossi, N. Rega, J.M. Millam, M. Klene, J.E. Knox, J.B. Cross, V. Bakken, C. Adamo, J. Jaramillo, R. Gomperts, R.E. Stratmann, O. Yazyev, A.J. Austin, R. Cammi, C. Pomelli, J.W. Ochterski, R.L. Martin, K. Morokuma, V.G. Zakrzewski, G.A. Voth, P. Salvador, J.J. Dannenberg, S. Dapprich, A.D. Daniels, Ö. Farkas, J.B. Foresman, J.V. Ortiz, J. Cioslowski, D.J. Fox, Gaussian 16 Revision, Gaussian, Inc. Wallingford (2016).

[8] P. Hohenberg, W. Kohn, Inhomogeneous Electron Gas, Physics Review **136** (1964) B864–B871. https://doi.org/10.1103/PhysRev.136.B864.

[9] C. Lee, W. Yang, R.G. Parr, Development of the Colle-Salvetti correlation-energy formula into a functional of the electron density, Physics Review B **37** (1988) 785–789. https://doi.org/10.1103/PhysRevB.37.785.

[10] R.G. Parr, W. Yang, Density-functional theory of atoms and molecules, 1. iss. as ... paperback, Oxford Univ. Press, New York, NY, 1994.

[11] A.D. Becke, Density-functional thermochemistry. III. The role of exact exchange, Journal of Chemical Physics, **98** (1993) 5648–5652. https://doi.org/10.1063/1.464913.

[12] T.H. Dunning, Gaussian basis sets for use in correlated molecular calculations. I. The atoms boron through neon and hydrogen, Journal Chemistry Physics, **90** (1989) 1007–1023. https://doi.org/10.1063/1.456153

[13] R. Dennington, T.A. Keith, Millam, M. John, GaussView 06 Semichem Inc., Shawnee Mission, KS (2016).

[14] E.D. Glendening, A.E. Reed, J.E. Carpenter, F. Weinhold, NBO 3.1 Gaussian Inc., Pittsburgh (2003).

[15] M.K. Chaudhary, A. Srivastava, K.K. Singh, P. Tandon, and B.D. Joshi. Computational evaluation on molecular stability, reactivity, and drug potential of frovatriptan from DFT and molecular docking approach. *Computational and Theoretical Chemistry,* **1191** (2020): 113031. https://doi.org/10.1016/j.comptc.2020.113031

[16] P.K. Weiner, R. Langridge, J.M. Blaney, R. Schaefer, P.A. Kollman, Electrostatic potential molecular surfaces, Proc. National Academy of Sciences, U.S.A.79 (1982) 3754–3758. https://doi.org/10.1073/pnas.79.12.3754

[17] A.E. Reed, L.A. Curtis, F.A. Weinhold, Intermolecular interactions from a natural bond orbital, donor-acceptor viewpoint, Chemcal Review, **88** (1988) 899–926. https://doi.org/10.1021/cr00088a005

[18] P. Geerlings, F.D. Proft, W. Langenaeker, Conceptual density functional theory, Chemical Review, 103 (2003) 1793−1874. https://doi.org/10.1021/cr990029p

[19] R.G. Parr, L. Szentpaly, S. Liu, Electrophilicity index, Journal of Amecan Chemical Society, **121** (1999)

1922−1924. https://doi.org/10.1021/ja983494x

[20] A. Daina, O. Michielin, V. Zoete, SwissTargetPrediction: updated data and new features for efficient prediction of protein targets of small molecules, Nucleic Acids Research, **47** (2019) W357–W364. https://doi.org/10.1093/nar/gkz382.

[21] P.W. Rose, B. Beran, C. Bi, W.F. Bluhm, D. Dimitropoulos, D.S. Goodsell, A. Prlic, M. Quesada, G.B. Quinn, J.D. Westbrook, J. Young, B. Yukich, C. Zardecki, H.M. Berman, P.E. Bourne, The RCSB Protein Data Bank: redesigned web site and web services, Nucleic Acids Research, **39** (2011) D392–D401. https://doi.org/10.1093/nar/gkq1021.